AD-A106 395 INDIANA UNIV AT BLOOMINGTON DEPT OF CHEMISTRY F/G 20/5
DETERMINATION OF ATOMIC AND MOLECULAR EXCITED-STATE LIFETIMES U--ETC(U)
OCT 81 R E RUSSO, G M HIEFTJE N00014-76-C-0838
UNCLASSIFIED TR-41 NL

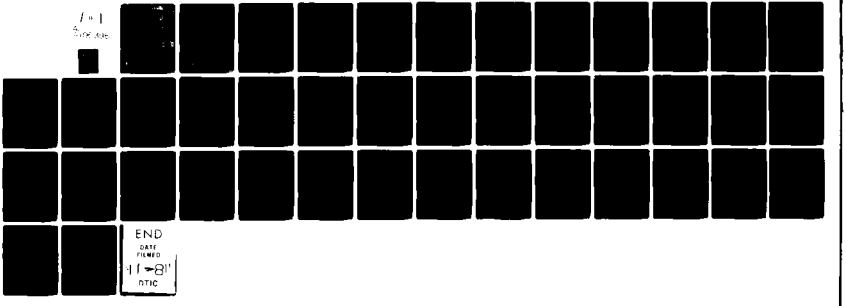

END
DATE FILMED
11-81
DTIC

UNCLASSIFIED

SECURITY CLASSIFICATION OF THIS PAGE (When Data Entered)

(12) LEVEL II

REPORT DOCUMENTATION PAGE

READ INSTRUCTIONS BEFORE COMPLETING FORM

1. REPORT NUMBER: FORTY-ONE	2. GOVT ACCESSION NO.: AD-A106 395
3. RECIPIENT'S CATALOG NUMBER: (14) TR-44	
4. TITLE (and Subtitle): Determination of Atomic and Molecular Excited-State Lifetimes Using an Opto-electronic Cross-correlation Method	5. TYPE OF REPORT & PERIOD COVERED: (9) Interim Technical Report
	6. PERFORMING ORG. REPORT NUMBER: 1599
7. AUTHOR(s): R. E. Russo and G. M. Hieftje	8. CONTRACT OR GRANT NUMBER(s): (15) N00014-76-C-0838
9. PERFORMING ORGANIZATION NAME AND ADDRESS: Department of Chemistry, Indiana University, Bloomington, IN 47405	10. PROGRAM ELEMENT, PROJECT, TASK AREA & WORK UNIT NUMBERS: NR 51-622
11. CONTROLLING OFFICE NAME AND ADDRESS: Office of Naval Research, Washington, D.C.	12. REPORT DATE: (11) Oct 1981
	13. NUMBER OF PAGES: 37
14. MONITORING AGENCY NAME & ADDRESS (if different from Controlling Office)	15. SECURITY CLASS. (of this report): UNCLASSIFIED
	15a. DECLASSIFICATION/DOWNGRADING SCHEDULE

16. DISTRIBUTION STATEMENT (of this Report)

This document has been approved for public release and sale; its distribution is unlimited.

DTIC ELECTE OCT 28 1981 B

17. DISTRIBUTION STATEMENT (of the abstract entered in Block 20, if different from Report)

18. SUPPLEMENTARY NOTES

Prepared for publication in APPLIED SPECTROSCOPY

19. KEY WORDS (Continue on reverse side if necessary and identify by block number)

Time-resolved fluorescence
Correlation
Atomic fluorescence
Laser-induced fluorescence
Transition probabilities

20. ABSTRACT (Continue on reverse side if necessary and identify by block number) A new optoelectronic cross-correlation technique has been employed to measure excited-state lifetimes of several organic fluorophores in solution and of sodium atoms in both air-acetylene and methane-air flames. Capable of time resolution in the picosecond range, the new method was validated by the excellent agreement between measured and literature values for fluorescence lifetimes of the organic species. Lifetime values for Na atoms in flames are among the most precise ever reported and agree closely with values calculated from the known flame gas composition, temperature, and the quenching cross-sections of the two dominant quenching species in the

DD FORM 1 JAN 73 1473 EDITION OF 1 NOV 65 IS OBSOLETE S/N 0102-014-6601

UNCLASSIFIED

SECURITY CLASSIFICATION OF THIS PAGE (When Data Entered)

20. Abstract (cont.)

flame, N_2 and CO_2. From the Na excited-state lifetimes (0.72 ± 0.07 ns for air-acetylene and 0.48 ± 0.08 ns for methane-air flames), quantum efficiencies for atomic fluorescence were calculated.

OFFICE OF NAVAL RESEARCH
Contract N00014-76-C-0838
Task No. NR 051-622
TECHNICAL REPORT NO. 41

DETERMINATION OF ATOMIC AND MOLECULAR EXCITED-STATE LIFETIMES USING AN OPTO-ELECTRONIC CROSS-CORRELATION METHOD

by

R. E. Russo and G. M. Hieftje

Prepared for Publication

in

APPLIED SPECTROSCOPY

Indiana University
Department of Chemistry
Bloomington, Indiana 47405

October 7, 1981

INTRODUCTION

Fluorescence lifetimes are valuable in chemical analysis in that they provide fundamental information about the flow of energy within an atom or molecule, about quenching processes, the kinetics of interatomic or intermolecular reactions, and many other physical and chemical processes (1-3). For example, one of the most important fundamental parameters in atomic spectrometry, the transition probability (A), is just the reciprocal of the fluorescence lifetime. The value of A affects the choice of a transition to be utilized for analysis and the accuracy of many critical measurements such as temperature and atomic concentration (4). However, most measurements of A are based on steady-state behavior and produce errors of 50% or more in experimentally determined values (4). Usually, far greater accuracy could be obtained through use of excited-state lifetimes.

Unfortunately, most measurement methods offer neither the time-resolution capability nor sensitivity necessary to measure nanosecond or picosecond lifetimes, especially for atomic systems which exhibit self-luminescence (i.e., emission). In the present study, a new method is employed which is useful for the determination of atomic excited-state lifetimes and which offers picosecond time-resolution and excellent sensitivity (5). In this method, a repetitive train of picosecond pulses generated by a synchronously pumped dye laser is used to excite the fluorophore (atoms or molecules) of interest. The decay time of the excited-state from this impulse excitation is measured by a novel opto-electronic cross-correlation technique (5), but with new instrumentation.

To verify the method and test the new instrument, the system was used to measure excited-state lifetimes of several organic compounds in solution: Rhodamine B; Rose Bengal; and Cresyl Violet. The measured lifetimes agreed well with those obtained with a sampling oscilloscope and to literature values, but were more precise.

Principal emphasis in this study was placed on the measurement of atomic lifetimes in analytical flames. Previous investigations of atomic fluorescence lifetimes in flames have been made using pulsed excitation sources, but with poor time resolution compared to the lifetime of the excited state (6); this is not the case with the present opto-electronic cross-correlation approach.

For the measurement of atomic systems, sodium was chosen as the primary element of study because its resonance lines (589.0) and 589.6 nm) overlap the peak spectral output (590 nm) of the available Rhodamine 6G (R6G) dye laser. The Na lifetime in the flame was measured as a function of flame-gas composition and spatial position within the flame. From the measured lifetime values, the quantum efficiency and cross-section for the collisional deactivation of the Na atoms with N_2 molecules were calculated, based on the known value for the natural radiative lifetime of Na (16.2 ns) and the established flame-gas composition. A brief account of quenching theory as it applies to excited atoms in the flame is included.

EXPERIMENTAL

Measurement of Excited-State Lifetimes. Time-resolved fluorescence decay curves were measured using a synchronously pumped dye laser for ex-

citation and a novel opto-electronic cross-correlation scheme for detection (cf. Fig. 1). The cross-correlation approach to fluorescence lifetime measurement offers several advantages over other techniques. A strong advantage of correlation in general is signal-to-noise (S/N) enhancement (7-8). In addition, excellent time-resolution and fast data acquisition are possible; the entire decay curve can be traced out in several seconds. Probably the most significant advantage is the ability to measure decay times of self-luminous samples, such as atoms in flame or plasma. Luminous samples suffer only a slight loss in signal-to-noise ratio caused by photodetector shot noise (8). The main components of the new instrument are described separately below.

Excitation Source-Synchronously Pumped Dye Laser (sync-pump). The ideal temporal pattern of an excitation source for use in time-resolved fluorimetry resembles a mathematical delta function (impulse). In this work, approximate "delta-function" pulses were provided by a synchronously pumped dye laser (9-21). The sync-pump provides high-power, 5-6 picosecond pulses of tunable radiation at pulse rates near 100 MHz. The characteristics of the particular laser system used in the present work are summarized in Table 1. The laser system was modified slightly in order to achieve the power stability cited in Table 1; this modification involved re-arrangement of the opto-electronic feedback network supplied with the Ar-ion laser (22).

Detection: Opto-Electronic Cross-Correlation Approach. The time-dependent fluorescence decay curve was recorded by an opto-electronic network constructed to measure the cross-correlation (8, 23-25) between the laser pulse and the resulting fluorescence waveform. In this particular

application, the cross-correlation performs a gating function, similar to a boxcar integration (26). After excitation by each laser pulse, the fluorescence radiation is monitored at 90° to the incident beam by means of a fast-response photomultiplier tube (PMT, Model 31024, RCA, Lancaster, PA). In addition, an electrical signal which mimics the time characteristics of the laser pulse is generated by a fast photodetector (PD, Model 403B, Spectra-Physics, Mountain View, CA) and multiplies the PMT output in a fast-response microwave mixer (Model ZFM-4, Mini Circuits, New York, NY). Therefore, the output of the mixer is a waveform which is zero except where both pulses are non-zero. At this point of overlap, the output is proportional to the product of the amplitudes of the laser-monitoring photodetector pulse and the fluorescence-monitoring PMT curve. Therefore, this product signal is a time-sampled representation of the fluorescence signal at one particular moment in its history (8). Time sampling occurs repetitively because of the repetitively pulsed nature of the laser output; accordingly, a time-averaged signal is obtained. Changing the relative arrival time of the pulses at the two detectors then causes a temporal shift of the two waveforms with respect to each other, permitting sampling at different points on the decay curve. Changing the relative arrival time of the pulses in the present instrument involves merely varying the optical path-length the pulses must travel before reaching either detector. The entire fluorescence decay curve can thus be traced out by smoothly varying this optical delay; the output signal level will reflect the change in the relative waveform position.

Microwave Mixer. The double-balanced microwave mixer (DBM) used in the new instrument (cf. Fig. 1) is simply a four-quadrant ring-diode multi-

plier (Fig. 2). The reference frequency (RF) and local oscillator (LO) inputs of the ZFM-4 mixer respond to frequencies in the 5 MHz - 1.25 GHz range. The output or intermediate frequency (IF) port provides the product of the input signals with a bandwidth from DC to 1.25 GHz. The DC frequency is essential to the cross-correlation approach since an average (DC) value is recorded.

In this device (cf. Fig. 1), the 403B photodiode signal was connected to the RF input of the mixer because this input offers better isolation and lower conversion loss at high frequencies than does the LO input (27). The electrical pulse from the PMT was connected to the LO input of the mixer. All connections to the mixer were made via RG58L coaxial cable (50 Ω) using GR-874 (Gen Rad, Concord, MA) connectors.

A constant-impedance, variable-length air-dielectric transmission line (Model 874-LK201, Gen Rad) was inserted between the 403B photodiode and the mixer to reduce the influence of reflections of electrical pulses along the line. Ideally, the length of the line should be adjusted so a reflected pulse overlaps the following original pulse (23). However, when such overlap occurs, distortion of the original pulse results. Accordingly, the length of the line was adjusted in the present study so each reflected pulse occurs (at the IF output) just before the next original pulse. The usable time range then stretches from the leading edge of the main pulse to the leading edge of the reflected pulse. For the sync-pump laser, this time period is approximately 11 ns, more than adequate for the studies herein.

Optical Delay Line. The optical delay used in the instrument of Fig. 1 offers higher time resolution and accuracy than typical electronic delay systems. Temporal accuracy is enjoyed because delay in position can be mea-

sured quite exactly and is related to delay in time by the speed of light. In addition, no problems arise from electronic jitter or triggering instability.

The optical delay was designed around a translatable corner-cube reflector (Fig. 3). The laser beam is directed onto one side of the corner-cube reflector; the reflector folds the beam back along a path parallel to the incoming radiation, but displaced from it by approximately 4 cm. Translation of the corner-cube in the direction of the laser beam then causes a change in optical path length and thus in the arrival time of the pulses at the sample cell, and subsequently of the fluorescence pulse at the PMT. The reflector is mounted on a movable platform attached at each end to a slide-wire. The wire stretches around two pulleys, one of which is mounted on the armature of a stepper motor (Model 34H-509A motor, Computer Devices, Sante Fe Springs, CA; SM-2A controller, Denco Research, Tucson, AZ), which can be operated under either manual or computer control. One-step resolution of the motor is equivalent to 0.5 mm movement of the corner-cube; total movement of the reflector is 1.9 m. These distances are doubled in the time domain because of the parallel beam path. Therefore, in temporal terms, resolution is 3 ps over a 12.4 ns delay range. The accuracy and precision in the corner-cube position were measured to be ± 2 steps over the entire delay range; i.e., ± 2 steps in 1900 steps (± 6 ps).

For computer operation of the delay line, the stepper motor was interfaced to a PDP-11/34 minicomputer (Digital Equipment Corp., Maynard, MA). A Fortran program allows interactive control of the delay resolution, total movement, and scan speed of the corner-cube.

Other Components. A rotating-sector chopper modulates the laser pulse train at a frequency of approximately 50 Hz. A lock-in amplifier (Model

840 Autoloc, Keithley Instruments, Cleveland, OH) was used as a low-pass filter to perform the averaging needed in the cross-correlation experiment. In this application, the detection bandpass is simply displaced from DC to the chopper frequency; problems arising from drift in the detection system are thereby eliminated. The reference signal for the lock-in amplifier was derived from a relatively slow response photodiode (XL56, Texas Instruments Co.) to which a portion of the laser beam was directed. The output of the lock-in amplifier was connected to an A/D channel of the PDP-11/34 computer.

Neutral density (ND) and variable neutral-density (VND) filters were used in several places in the beam path to control the light level reaching the various detectors. A narrow-band interference filter (IF) was employed between the sample cell and PMT to minimize detection of background light or, in the molecular fluorescence experiments, of scattered or stray laser radiation.

The PMT was operated at -2700 V, chosen on the basis of a tradeoff between response time and rms noise. At this voltage, the response time of the PMT was found to be 1.1 ns FWHM and essentially constant over the tunable wavelength range of the R6G dye laser. Therefore, no response-time correction factor is required in non-resonance luminescence measurements (28,29).

Sampling Oscilloscope. Fluorescence lifetimes measured with the cross-correlation technique were validated by comparison with results obtained with a sampling oscilloscope (Model 7T11 sampling sweep unit; Model 7S11 sampling unit with Model S-4 sampling head, Model 7844 plug-in main frame, Tektronix, Beaverton, OR). The photoelectric pulse from the XL56 photodiode

usually used as a reference for the lock-in amplifier provided a stable trigger for the oscilloscope. Fluorescence was detected by the RCA 31024 PMT which was connected directly to the oscilloscope sampling head (Model S-4, Tektronix). In this way, the best impedance match between the PMT and sampling head was obtained and the least pulse distortion generated. The horizontal time-base of the oscilloscope was driven externally by a linear voltage ramp (0-10 V) from the PDP-11/34 computer. Using the oscilloscope in this way would initially seem to provide time resolution defined by the oscilloscope horizontal time scale setting (usually 1 ns/div) divided by 4096 (the resolution of the D/A converter employed to drive the time base). However, because of remaining system noise and trigger jitter, the actual resolution was substantially poorer ($\geq$ 20 ps). The vertical amplifier of the oscilloscope was connected directly to an A/D input of the computer. A Fortran program was used to generate the horizontal voltage sweep and to simultaneously record the voltage level from the vertical amplifier. Resolution and number of scans could be preset interactively.

The fluorescence lifetimes of several organic compounds in solution were measured. The particular species studied were Rhodamine B (RB), Rose Bengal (Rose), and Cresyl Violet (CV), each dissolved in ethanol at a concentration of 1×10^{-6} M. A glass cuvette was used as the sample cell for these solutions. Table 2 lists the excitation wavelength, detection wavelength and interference filter used for each fluorophore.

When atomic fluorescence was investigated, atoms were generated in air-acetylene and natural-gas air flames, both supported on an Alkemade-type burner. A fritted glass bubbler was employed for nebulization of analyte solution into the flame. Three different gas compositions were employed

for Na fluorescence measurements in the air-acetylene flame: fuel-rich (F/O = 0.14); fuel-lean (F/O = 0.12); and stoichiometric (F/O = 0.13). In addition, the Na lifetime was measured at four separate horizontal locations in the flame: in the radial center, 3 mm from center, 6 mm from center, and at the flame edge (8 mm from center). Finally, the Na fluorescence lifetime was measured at the outside edge of a natural gas-air flame, a region where thermal (background) emission was nearly absent.

RESULTS AND DISCUSSION

Molecular Excited-State Lifetimes. An example of the instrument response and measured and calculated (convoluted) fluorescence decay curves are shown in Fig. 4 for a 1 μM cresyl violet solution. The measured fluorescence decay curve is distorted by the finite duration of the excitation pulse and by the limited bandwidth of the detection system. Specifically, the measured decay curve is the convolution (30-33) of the actual fluorescence decay curve, the excitation pulse shape, and the detection system response function; the latter two constitute the overall instrument response function. Therefore, the measured fluorescence pulse must be deconvolved with the instrument response function to yield an accurate value for the fluorescence decay lifetime. To achieve this goal, a convolute-and-compare method was employed in this work and is based on a discrete, computer-adaptable serial product method (34) for convolving two functions. In the convolute-and-compare technique, the fluorescence decay is assumed to be an exponential function (1,30,35) which is then mathematically convolved with the measured instrumental response curve. The resulting calculated fluorescence curve

is compared to the measured fluorescence decay waveform and the sum of the squares of the residuals between the two curves is computed. The decay rate constant is iteratively varied by the computer until the residuals are minimized. In this work, a simplex (36) optimization procedure was employed to minimize the residuals.

For the 1 μM cresyl violet solution (cf. Fig. 4), the lifetime determined by this procedure was 3.48 ns, in satisfactory agreement with the calculated and measured fluorescence response curves. The secondary pulse seen at the end of the time range in Fig. 4 results from electrical reflections in the line between the fast photodiode (403B) and the microwave mixer, but does not distort the measurement during the earlier, important part of the curve.

Table 3 compares cited molecular lifetimes to those measured using the cross-correlation and sampling oscilloscope methods. Lifetimes obtained by the cross-correlation approach are in good agreement with those obtained previously using the same technique (23,37). However, the lifetimes measured with the sampling oscilloscope are consistently higher than those obtained with the cross-correlation system. Possible explanations for the longer lifetimes determined with the sampling oscilloscope are incorrect horizontal time-scale and triggering jitter. The precision of the cross-correlation system is shown to be much better than that of the sampling oscilloscope. Moreover, the precision obtained with the sampling oscilloscope is better here than usually found because the time base and vertical amplifier was computer-controlled and S/N was improved by averaging 200-300 repetitions.

Atomic Lifetimes. The measured instrument response and fluorescence decay, and the calculated (convoluted) fluorescence decay for Na in the stoichiometric (F/O = 0.13) air-acetylene flame are shown in Fig. 5. Fluo-

rescence was observed approximately 5 cm above the burner top where desolvation and vaporization should be complete, where Mie scattering is minimized, and where the flame can be safely assumed to be in thermodynamic equilibrium. Five separate measurements of the fluorescence decay curve were obtained, and each compared to the calculated fluorescence decay curve. A weighted average for the five determinations was calculated (40) and found to be 0.72 ± 0.07 ns. Within experimental error, this same lifetime was measured for 1, 25, and 50 ppm NaCl solutions introduced into the flame, indicating that radiation-trapping effects are negligible. Significantly, the Na lifetime in the flame measured in this work is the only value below 1 ns ever reported with good precision.

Comparison of Measured and Calculated Na Fluorescence Lifetimes. As expected, the Na lifetime measured in the air-supported flame is substantially less than the 16.2 ns natural radiative lifetime (6,41,42) because of excited-state quenching by flame-gas molecules (43). Quenching occurs because the rates of collisional deactivation by the most abundant flame gas molecules are much greater than atomic radiative decay rates (42,43).

In general, the deactivation rate of the excited state can be described as (1,35,44-46)

$$k_F = k_o + \sum_x k_x \qquad (1)$$

where k_F is the measured fluorescence decay rate (reciprocal of the lifetime), k_o is the natural radiative decay rate, and $\sum_x k_x$ is the sum of rates for all collisional processes of species x in the flame which deactivate the excited atoms. Equation 1 can be expressed in terms of the measured (τ_F) and natural

(τ_o) radiative lifetimes as

$$\tau_F^{-1} = \tau_o^{-1} + \sum_x k_x \tag{2}$$

Quenching rate constants k_x are generally expressed in terms of quenching cross-sections σ^2, defined as the square of the distance between the centers of the two colliding species. The summation rate constant of equations 1 and 2 is related to the quenching cross-section by (45,46).

$$\sum_x k_x = \sum_x n_x \bar{g}_x \sigma_x^2 \quad \text{sec}^{-1} \tag{3}$$

where n_x is the number density (in cm^{-3}) of quenching species x, $\bar{g}_x$ is the average relative velocity (in cm/sec) of the colliding atom and quenching species x, and the cross-section σ^2 is expressed in cm^2. Furthermore, n_x and $\bar{g}_x$ are given by (45,46).

$$n_x = P_x/kT \tag{4}$$

$$\bar{g}_x = (8kT/\pi\mu_x)^{1/2} \tag{5}$$

where P_x is the partial pressure (in atmospheres) of flame species x, k is the Boltzmann constant (erg/K), T is the absolute temperature (Kelvin), and μ_x is the reduced mass (g/mole) of the atom and species x. Therefore, from a known flame-gas composition and temperature, and known quenching cross-section of each important flame species, fluorescence lifetimes can be calculated and compared with measured values. Atlernatively, if a single

flame species is assumed to be primarily responsible for quenching, a measured fluorescence lifetime can be used to calculate the cross-section for that species. Finally, if the flame composition is varied, the quenching cross-sections for several intrinsic flame species can be determined from the observed changes in the fluorescence lifetime.

If a flame is considered to be in thermodynamic equilibrium, its temperature can readily be measured (47,48) and its chemical composition can be calculated from the measured temperature, the unburnt gas mixture and known flame reactions (43,48). Computer-based algorithms are commonly employed for these calculations (43,49); calculated compositions of the stoichiometric air-acetylene flame are presented in Table 4 (48,50). The molecules listed in Table 4 are the major species responsible for quenching in the flame; the dominance of the N_2 component is evident. The partial pressure of O_2, H_2, and OH are so low that their effects are usually neglected in most calculations of quenching (46). Similarly, quenching by free radicals or flame electrons is assumed to be negligible because of their low concentrations in the secondary combustion zone of the flame (45,51). Finally, the frequency of ternary collisions between an excited-state atom and two flame molecules is approximately three-to-four orders of magnitude smaller than binary collisions and can also be neglected (51).

In the experimental determination of quenching cross-sections for individual flame-borne molecules, a series of isothermal flames with different gas compositions must be produced and the overall quenching rate constant measured in each flame. In particular, one needs x different flame compositions, where x is the number of quenching species that are to be considered (cf. equation 3). However, because N_2 is the primary species present in

an air-supported atmospheric-pressure flame, an approximate collisional cross-section can be obtained for N_2 by assuming that the excited atoms collide solely with N_2 molecules (52). For Na atoms in the air-acetylene flame, the quenching rate constant (cf. equations 3, 4, and 5) can then be expressed as

$$\sum_x k_x \simeq k_{N_2} = (P_{N_2}/kT)(8kT/\pi\mu_{Na-N_2})^{1/2}\ \sigma^2_{Na-N_2} \qquad (6)$$

Table 5 compares measured excited-state lifetimes and those calculated using Eqs. 2-6 to results of other studies. Also shown are the quenching cross-sections for N_2 on Na calculated from Eq. 6. Literature values for the partial pressures and quenching cross-sections of N_2 and CO_2 used in Eq. 6 to calculate the Na lifetime are listed in Tables 4 and 5, respectively. In this work, the Na lifetime was calculated assuming first that N_2 molecules are solely responsible for quenching and then that both N_2 and CO_2 molecules contribute to quenching. Although the first assumption is commonly used (54) because N_2 is the predominant flame-gas species (cf. Table 4), the contribution to quenching of Na by CO_2 will be significant because of its relatively high partial pressure (cf. Table 4) and large cross-section (cf. Table 5). From Table 5, the Na fluorescence lifetime measured in this work is in good agreement with the expected theoretical value, especially when the contribution to quenching by CO_2 is considered.

This argument is supported by the approximate quenching cross-section for N_2 on Na which was calculated from the measured lifetime using Eq. 6. Because Na was assumed to be the only species responsible for quenching, the resulting value (25.2 $\mathring{A}^2$) is higher than others which have been reported.

Remaining disparities among the values in Table 5 can be attributed to several factors. The partial pressures listed in Table 4 pertain to a stoichiometric air-acetylene flame with a temperature of 2500 or 2600 K; the line-reversal temperature for the flame employed in the present studies was measured to be 2350 K. In addition, the reported quenching cross-sections are assumed to be constant over a temperature range of 1500-2500 K. For N_2, this assumption has been validated (46), although not for CO_2. Quenching cross-sections, in general, will decrease with increasing temperature (46,56). For most molecular species in Table 4 other than N_2, the cited cross-sections are believed to be larger than they would be at the air-acetylene flame temperature (58).

Quantum Efficiency. Quantum efficiency is an important factor in determining the utility of a particular flame for atomic fluorescence spectrometry. Traditionally, quantum efficiencies in flames have been determined from the ratio of the total radiant power fluoresced over a given solid angle to the total resonantly absorbed radiant power (6,56,59-63). However, this absolute method is often unreliable because of uncertainties in the solid angle of detection, anisotropy in the angular distribution of the fluorescence radiation, and non-resonant absorption and re-emission in the flame (6,56). In addition, the fluorescence radiance emerging from the flame can be lower than that emitted by the atoms in the path of the exciting beam because of post-filter effects (6,51,56).

A more direct determination of quantum efficiency involves measurement of the excited-state lifetime in the flame. This approach is based on the fact that quantum efficiency (Q_F) is just the ratio of the intrinsic excited-state decay rate (k_o) to the total decay rate (k_F):

$$Q_F = k_o/k_F \quad (7)$$

In turn, because the decay rate is the reciprocal of the lifetime, quantum efficiency can be expressed in terms of the measured (τ_F) and spontaneous (τ_o) excited-state lifetimes by

$$Q_F = \tau_F/\tau_o \quad (8)$$

From the fluorescence lifetime value reported in Table 5, the fluorescence quantum efficiency measured in this work is in excellent agreement with earlier results (6,55).

Effect of Spatial Position in the Flame on Fluorescence Lifetime. The well defined laser beam used here simplified the spatially resolved measurement of Na fluorescence lifetimes. The results of four localized measurements are shown in Fig. 6. The measured reduction in fluorescence lifetime indicates the effect of entrained atmospheric gases on the quenching of Na in the flame. It is believed that this decrease is caused largely by the presence of atmospheric oxygen; however, an increase in CO_2 concentration generated by secondary combustion might contribute. Similar behavior was observed for the H_2-O_2 flame (6, 54), although the spatial dependence of the fluorescence lifetime was more marked than in the air-acetylene flame. In the H_2-O_2 flame, the main cause of quenching is from N_2 entrainment, which accounts for a sharper decrease in the spatial dependence of the Na lifetime. In contrast, only when the fluorescence lifetime is measured at the edge of the air-acetylene flame is the lifetime significantly shorter than in the flame center.

Effect of Flame-Gas Composition on Fluorescence Lifetimes. The Na excited-state lifetime was measured at three different gas compositions: stoichiometric (F/O = 0.13), slightly fuel-lean (F/O = 0.12), and slightly rich (F/O = 0.14). These compositions were chosen to maintain a nearly constant flame temperature and were obtained by varying the acetylene flow. The Na excited-state lifetime in the lean flame was measured to be 0.67 ns and in the rich flame to be 0.65 ns. Importantly, the lifetime values for all three flame conditions fall within the precision (0.07 ns) of the measurement technique, and a statistical analysis of the values shows the difference not to be significant.

Natural Gas-Air Flame. A fluorescence lifetime of 0.48 ± 0.08 ns was measured for Na in a natural gas-air flame (cf. Fig. 7). This low value would ordinarily be surprising for this flame whose temperature is in the 1500 K range. However, the measurement was obtained outside the visible flame boundary where air entrainment is substantial. The lifetime was recorded at this location because it was the only place where Na fluorescence was strong and where thermal emission (background) was absent. Because of the low flame temperature, atom formation was not complete until approximately 10 cm above the burner top, although some atoms were present at the flame edge at a height of 4 cm, the measurement location in the flame.

CONCLUSION

Although the conventional time-correlated single-photon technique offers picosecond resolution and single photon sensitivity, it cannot be used to measure atomic lifetimes in analytical flames. In addition, the sampling

oscilloscope was found in this study to be incapable of measuring the weak Na fluorescence signal resulting from excitation by the relatively low-power synchronously pumped dye-laser. However, the opto-electronic cross-correlation technique appears to be suited for these sensitive fluorescence lifetime measurements.

The low power of the sync-pump dye-laser system renders frequency doubling very inefficient. Consequently, this laser cannot easily be used to obtain fluorescence lifetimes in the UV spectral region, where most elements exhibit strong resonance lines. Clearly, a higher laser power is desirable. In addition to increasing its utility for UV measurements, a higher laser power would enable the measurement of fluorescence lifetimes in strongly emitting sources, such as the ICP. Such measurements would provide a good method of determining quantum efficiency, a parameter which has not yet been characterized in plasmas.

ACKNOWLEDGEMENTS

We wish to thank Ralph Lemke for his considerable assistance in designing the computer programs for this work. This work was supported in part by the National Institutes of Health through grant PHS GM 24473, by the National Science Foundation through grant CHE 80-25633, and by the Office of Naval Research.

REFERENCES

1. A. J. Pesce, C. G. Rosen, and T. L. Pasby, Fluorescence Spectroscopy (Marcel Dekker, New York, NY, 1971).
2. J. B. Brinks and T. H. Monroe, Progr. Reaction Kinetics 4, 239 (1967).
3. R. D. Spencer and G. Weber, J. Chem. Phys. 52, 1654 (1970).
4. R. J. Brown and M. L. Parsons, Spectrochim. Acta 33B, 777 (1978).
5. J. M. Ramsey, G. M. Hieftje, and G. R. Haugen, Appl. Optics 18, 1913 (1979).
6. P. Hannaford, "XXI Colloquium Spectroscopicum Internationale and Eighth International Conference on Atomic Spectroscopy, Cambridge, England", Ch. 19 (Heyden and Sons, Ltd., London, 1979).
7. K. R. Betty and G. Horlick, Anal. Chem. 48, 1899 (1976).
8. G. M. Hieftje and G. Horlick, Amer. Lab 13, 76 (1981).
9. C. K. Chan and S. O. Sari, Appl. Phys. Lett. 25, 403 (1974).
10. H. Mahr and M. D. Hirsch, Opt. Commun. 13, 96 (1975).
11. J. M. Harris, R. W. Chrisman, and F. E. Lytle, Appl. Phys. Lett. 26, 16 (1975).
12. C. K. Chan, S.O. Sari, and R. E. Foster, J. Appl. Phys. 47, 1139 (1976).
13. J. deVries, D. Bebelaar, and J. Langelaar, Opt. Commun. 18, 24 (1976).
14. I. S. Ruddock, W. Sibbert, and D. J. Bradley, Opt. Commun. 18, 26 (1976).
15. E. P. Ippen and C. V. Shank, Opt. Commun. 18, 27 (1976).
16. S. L. Shapiro, Ultrashort Light Pulses (Springer-Verlag, NY,1976).
17. N. J. Frigo, T. Daby, and H. Mahr, IEEE J. Quantum Electron. QE-13, 101 (1977).
18. Z. A. Yasa, A. Dienes, and J. R. Whinnery, Appl. Phys. Lett. 30, 24 (1977).

19. J. P. Heritage and R. K. Jain, Appl. Phys. Lett. 32, 101 (1978).

20. A. I. Ferguson, J. N. Eckstein, and T. W. Haensch, J. Appl. Phys. 49, 5389 (1978).

21. J. Kuhl, H. Klingenberg, and D. von der Linde, Appl. Phys. 18, 279 (1979).

22. R. E. Russo, R. Withnell, and G. M. Hieftje, Rev. Sci. Instrum. 52, 772 (1981).

23. J. M. Ramsey, Ph.D. Thesis, Indiana University, 1979.

24. E. O. Brigham, The Fast Fourier Transform (Prentice Hall, Englewood Cliffs, NJ, 1974).

25. G. Horlick and G. M. Hieftje, "Correlation Methods in Chemical Data Measurements", in Contemporary Topics in Analytical and Clinical Chemistry, D. M. Hercules, G. M. Hieftje, L. R. Snyder, and M. A. Evenson, Eds. (Plenum Press, New York, NY, 1978), Vol. 3, Chap. 4.

26. G. M. Hieftje, Anal. Chem. 44(7), 69A (1972).

27. Mini-Circuits; Microwave Components and Accessories EEM Catalog, p. 2775, 1979.

28. D. M. Rayner, A. E. McKinnon, and A. G. Szabo, Rev. Sci. Instrum. 48, 1050 (1977).

29. B. Sipp, J. A. Mieke, and L. Delgado, Opt. Commun. 16, 202 (1976).

30. W. R. Ware, "Transient Luminescence Measurements", in Creation and Detection of the Excited-State, A. A. Lamola, Ed. (Marcel Dekker, New York, NY, 1971), Vol. 1A.

31. M. Ch. Studer, U. P. Wild, and H. Gunthard, J. Phys. E. 3, 847 (1970).

32. U. P. Wild, A. R. Holzwarth, and H. P. Good, Rev. Sci. Instrum. 48, 1621 (1977).

33. W. R. Ware, L. J. Doemeny, and T. L. Nemzek, J. Phys. Chem. 77, 2038 (1973).

34. R. N. Bracewell, The Fourier Transform and its Application, 2nd ed. (McGraw-Hill, New York, NY, 1978).

35. A. C. G. Mitchell and M. W. Zemansky, in Resonance Radiation and Excited-State Atoms (University Press, Cambridge, 1961).

36. J. P. Chandler, Fortran Program called STEPIT-performs the Simplex optimization, obtained through the Quantum Chemistry Program Exchange (QCPE), Department of Chemistry, Indiana University, Bloomington, IN, 1975.

37. G. M. Hieftje, G. R. Haugen, and J. M. Ramsey, Appl. Phys. Lett. 30, 463 (1977).

38. J. M. Harris and F. E. Lytle, Rev. Sci. Instrum. 48, 1469 (1977).

39. I. B. Berlman, Handbook of Fluorescence Spectra of Aromatic Molecules (Academic Press, New York, NY, 1971).

40. H. D. Young, Statistical Treatment of Experimental Data (McGraw-Hill, New York, NY, 1962).

41. C. Bastlein, G. Baumgartner, and B. Brosa, Z. Phys. 218, 319 (1969).

42. J. M. Daily and C. Chan, Combust. Flame 33, 47 (1978).

43. D. R. Jenkins and T. M. Sugden, "Radicals and Molecules in Flame Gases", in Flame Emission and Atomic Absorption Spectrometry, J. A. Dean and T. C. Rains, Eds. (Marcel Dekker, New York, NY, 1969), Vol. 1, Theory, Chap. 5.

44. J. R. Barker and R. E. Weston, Jr., J. Chem. Phys. 65, 1427 (1976).

45. D. R. Jenkins, Spectrochim. Acta 23B, 167 (1967).

46. P. L. Lijnse and R. J. Elsenaar, J. Quant. Spectrosc. Radiat. Transfer 12, 1115 (1972).

47. W. Snelleman, "The Measurement and Calculation of Flame Temperatures", in Flame Emission and Atomic Absorption Spectrometry, J. A. Dean and T. C. Rains, Eds. (Marcel Dekker, New York, NY, 1969), Vol. 1, Theory, Chap. 7.

48. A. G. Gaydon and H. G. Wolfhard, Flames, Their Structure, Radiation and Temperature, 4th ed. (Chapman and Hall, New York, NY, 1979).

49. P. J. Th. Zeegers, Ph.D. Thesis, University of Utrecht, 1966.

50. C. Th. J. Alkemade and R. Herrmann, Fundamentals of Analytical Flame Spectroscopy (John Wiley and Sons, New York, NY, 1979).

51. K. J. Laidler, The Chemical Kinetics of Excited-States (Oxford University Press, 1955), Chap. 2.

52. R. P. Lucht and N. M. Laurendeau, Combust. Flame 34, 215 (1979).

53. D. R. de Olivares, Ph.D. Thesis, Indiana University, 1976.

54. N. S. Ham and P. Hannaford, J. Phys. B: Atom Molec. Phys. 12, L199 (1979).

55. D. R. Jenkins, Spectrochim. Acta 25B, 47 (1970).

56. D. R. Jenkins, Proc. Roy. Soc. A 293, 493 (1966).

57. H. P. Hooymayers and P. L.Lijnse, J. Quant. Spectrosc. Radiat. Transfer 9, 995 (1969).

58. C. Th. J. Alkemade and P. J. Th. Zeegers, "Excitation and De-Excitation Processes in Flames", in Spectrochemical Methods of Analysis, J. D. Winefordner, Ed. (Wiley Interscience, John Wiley and Sons, New York, NY, 1971), Vol. 9.

59. D. R. Jenkins, Proc. Roy. Soc. A 303, 453 (1968).

60. D. R. Jenkins, Proc. Roy. Soc. A 303, 467 (1968).

61. D. R. Jenkins, Proc. Roy. Soc. A 306, 413 (1968).

62. H. P. Hooymayers and C. Th. J. Alkemade, J. Quant. Spectrosc. Radiat. Transfer 6, 501 (1966).

63. H. P. Hooymayers and C. Th. J. Alkemade, J. Quant. Spectrosc. Radiat. Transfer 6, 847 (1966).

Table 1. Characteristics of Synchronously Pumped Dye Laser System

Mode-locked Ar^+ Laser (Pump) (Model 171-06, Ar ion laser; Model 342 mode-locker with Model 452 mode-locker driver, Spectra-Physics, Mountain View, CA)

Wavelength	5145 Å
Pulse width	170 ps
Pulse repetition rate	82 MHz
Power Stability:	
light control	± 0.5 %
current control	± 4 %
Mode spacing with prism	83.3 - 86.2 MHz
Power at 5145 Å (30 Amps)	
CW	1.8 W
Mode locked	600 mW
Mode locker frequency	40.9400 MHz

Sync-Pump Dye Laser (Model 375 dye laser, Model 341 synchronous pumping accessory package, Spectra-Physics, Mountain View, CA)

Dye - Rhodamine 6G	(1.5 mM)
Tunable wavelength range	570 - 630 nm
Pulse width	5 - 7 ps
Pulse repetition rate	82 MHz
Average power	130 mW @ 590 nm
Duty cycle	5×10^{-4}
Stability:	
light control	1%
current control	6%

Table 2. Spectral Region of Study: Excitation Wavelength, Detection Wavelength, and Interference Filter

Fluorophore	*Excitation Wavelength(nm)	Detection Wavelength(nm)	**Detection Filter Bandpass Maximum(nm)
Na	589	589	590
Rhodamine B	560	590	560/590
Rose Bengal	560	580	560/580
Cresyl Violet	601	630	600/630

*Laser Bandwidth approximately 0.2 - 0.3 nm

**All filters have 10 nm bandpass

Table 3. Fluorescence Lifetimes of Molecular Species in Solution (1 μM in EtOH) (ns)

Fluorophore	Cross-Correlation Detection	Sampling Oscilloscope Detection	Literature Values	References
Rose Bengal	0.70 ± 0.02	0.78 ± 0.17	0.828 ± 0.017 0.7	(23) (37)
Rhodamine B	2.79 ± 0.09	2.94 ± 0.45	2.72 ± 0.03 2.88 3.2	(23) (38) (39)
Cresyl Violet	3.48 ± 0.11	3.82 ± 0.56	3.6	(39)

Table 4. Calculated Chemical Composition of Stoichiometric Air-Acetylene Flame

Flame-Gas Component	Partial Pressure (atm) at T=2500 K (48)	Partial Pressure (atm) at T=2600 K (50)
H_2O	0.07	0.08
CO_2	0.12	0.09
CO	0.04	0.1
O_2	0.02	0.01
H_2	0.00	0.01
OH	0.01	--
H	0.00	--
O	0.00	--
NO	0.01	--
N_2	0.73	0.69

Table 5. Measured, Calculated and Literature Values for Lifetime, Quantum Efficiency and Quenching Cross-Section for Na in a Stoichiometric Air-acetylene Flame

Parameter	This Work		Other	
	Measured	Calculated	Measured	Calculated
Fluorescence Lifetime (ns)	0.72 ± 0.07	0.89[1] 0.69[2]	1.0 (53) < 1 (54)	0.8 (54)[1]
Quantum Efficiency	0.044	0.055[1,3] 0.043[2,3]	0.049 (6)	0.042 (55)
Quenching Cross-Section				
σ_{Na-N_2} ($\AA^2$)		25.2[1]	22.2 (46)	14.1 (6) 21.5 (56)
σ_{Na-CO_2} ($\AA^2$)				54 (56) 50 (57)

[1]Calculated assuming $Na-N_2$ collisions solely responsible for quenching deactivation.

[2]Calculated assuming $Na-N_2$ and $Na-CO_2$ collisions both contribute to quenching deactivation.

[3]Based on known natural radiative lifetime of 16.2 ns.

FIGURE CAPTIONS

Figure 1. Block diagram of experimental system employed for time-resolved fluorescence measurements. PD, fast photodiode; BS, beam splitter; M, mirrors; PMT, photomultiplier tube; R, reference frequency input to mixer; L, local oscillator input to mixer; I, intermediate frequency output of mixer.

Figure 2. Diagram of double-balanced microwave mixer used in the cross-correlation experiment. PMT, photomultiplier tube; PD, photodiode; LO, local oscillator input; IF, intermediate frequency output; and RF, reference frequency input.

Figure 3. Diagram of experimental arrangement for optical delay line employed in the opto-electronic cross-correlation instrument.

Figure 4. Measured and calculated (convoluted) fluorescence response curves for a 1 μM cresyl violet solution in ethanol. A, instrument response function; B, measured fluorescence response curve; and C, convoluted fluorescence response curve. Measured lifetime - 3.48 ns.

Figure 5. Measured and convoluted atomic fluorescence response curves for Na in an air-acetylene flame. A, instrument response function; B, measured fluorescence response curve; and C, convoluted fluorescence response curve. Measured lifetime - 0.72 ns.

Figure 6: Excited-state lifetime versus radial flame position for Na. Vertical distance from burner top = 5 cm.

Figure 7. Measured and convoluted atomic fluorescence response curves for Na in a natural gas-air flame. A, instrument response function; B, measured fluorescence response curve; and, C, convoluted fluorescence response curve. Measured lifetime - 0.48 ns.

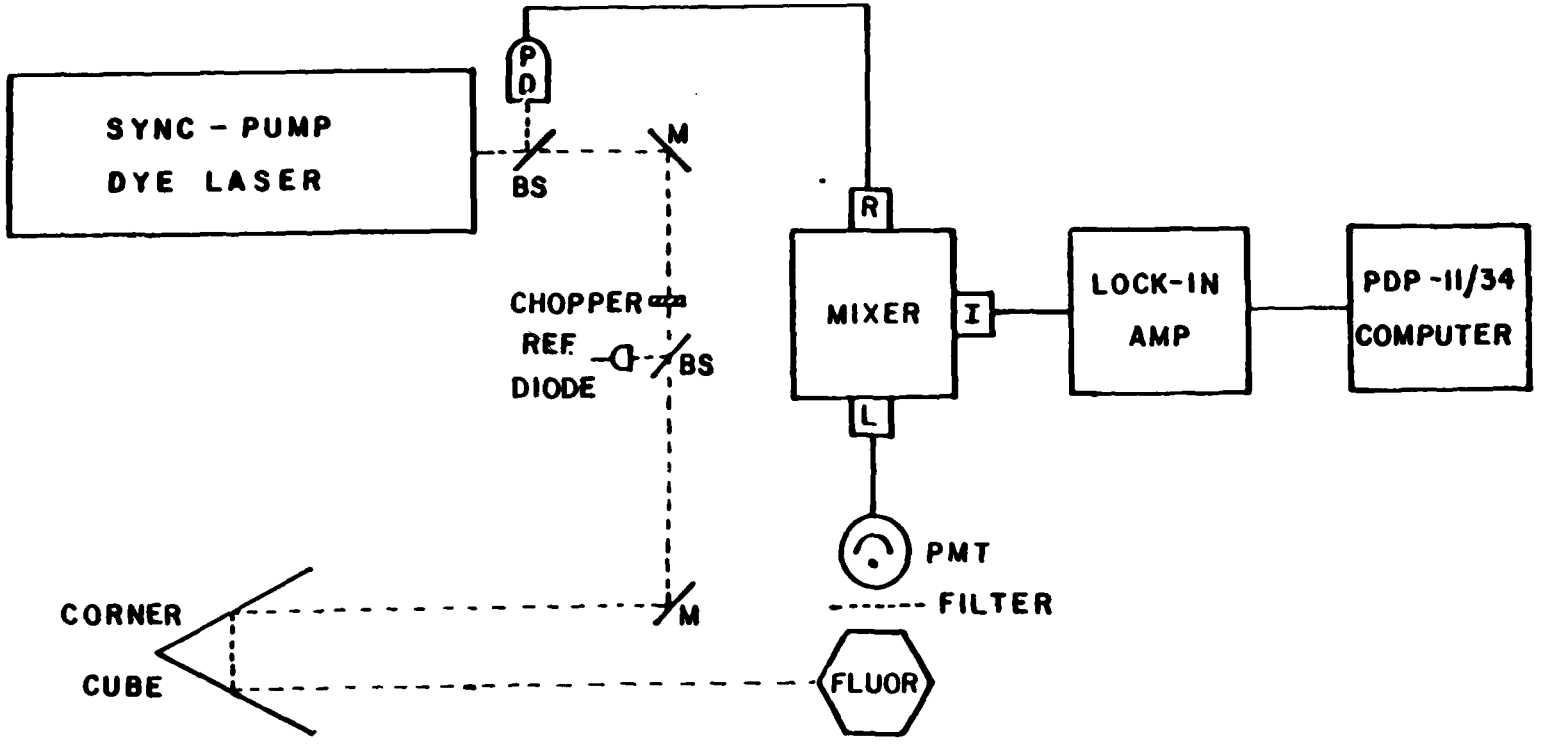
SYNC - PUMP
DYE LASER
PD
BS
M
CHOPPER
REF.
DIODE
BS
R
MIXER
I
L
LOCK-IN
AMP
PDP-11/34
COMPUTER
PMT
FILTER
M
CORNER
CUBE
FLUOR

Fig. 1

MIXER

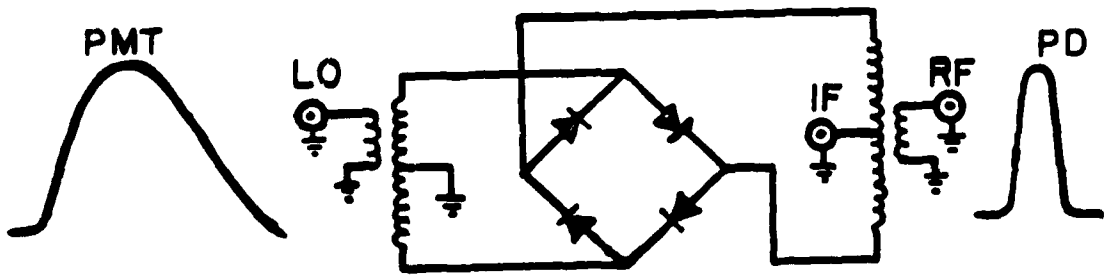

LO 5MHz - 1.2 GHz

RF 5MHz - 1.2 GHz

IF DC - 1.2 GHz

Fig. 2

VARIABLE OPTICAL DELAY

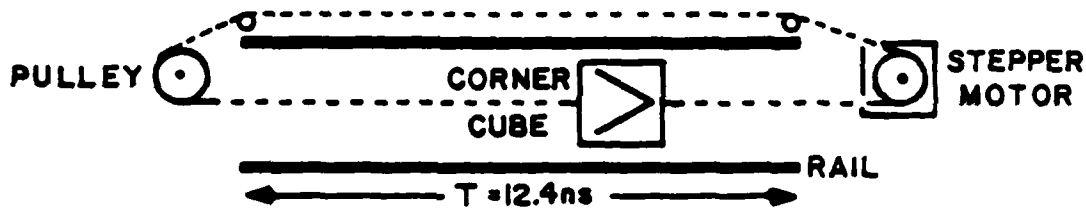

Fig. 3

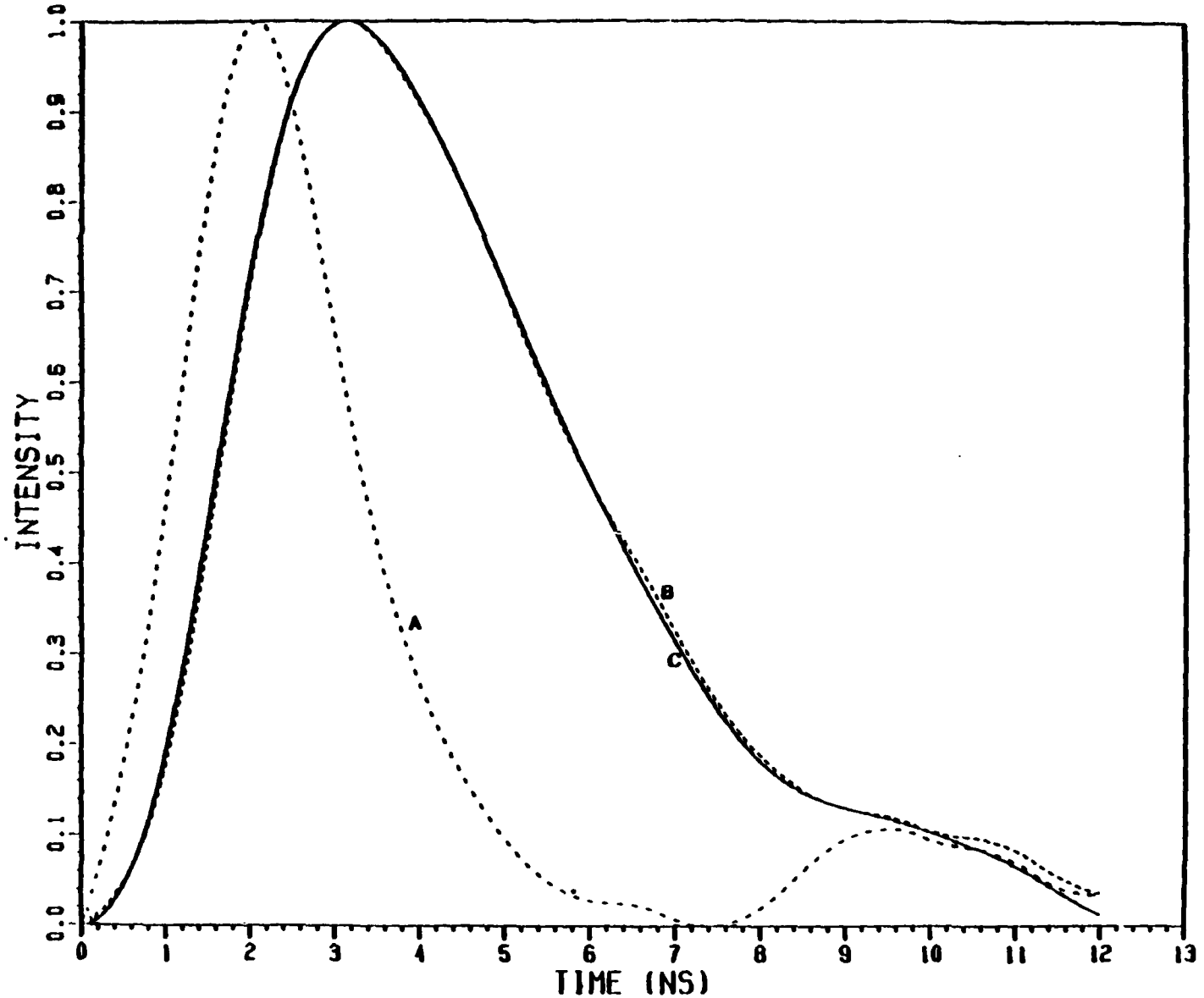
INTENSITY
0.0
0.1
0.2
0.3
0.4
0.5
0.6
0.7
0.8
0.9
1.0
0
1
2
3
4
5
6
7
8
9
10
11
12
13
TIME (NS)
A
B
C

Fig. 4

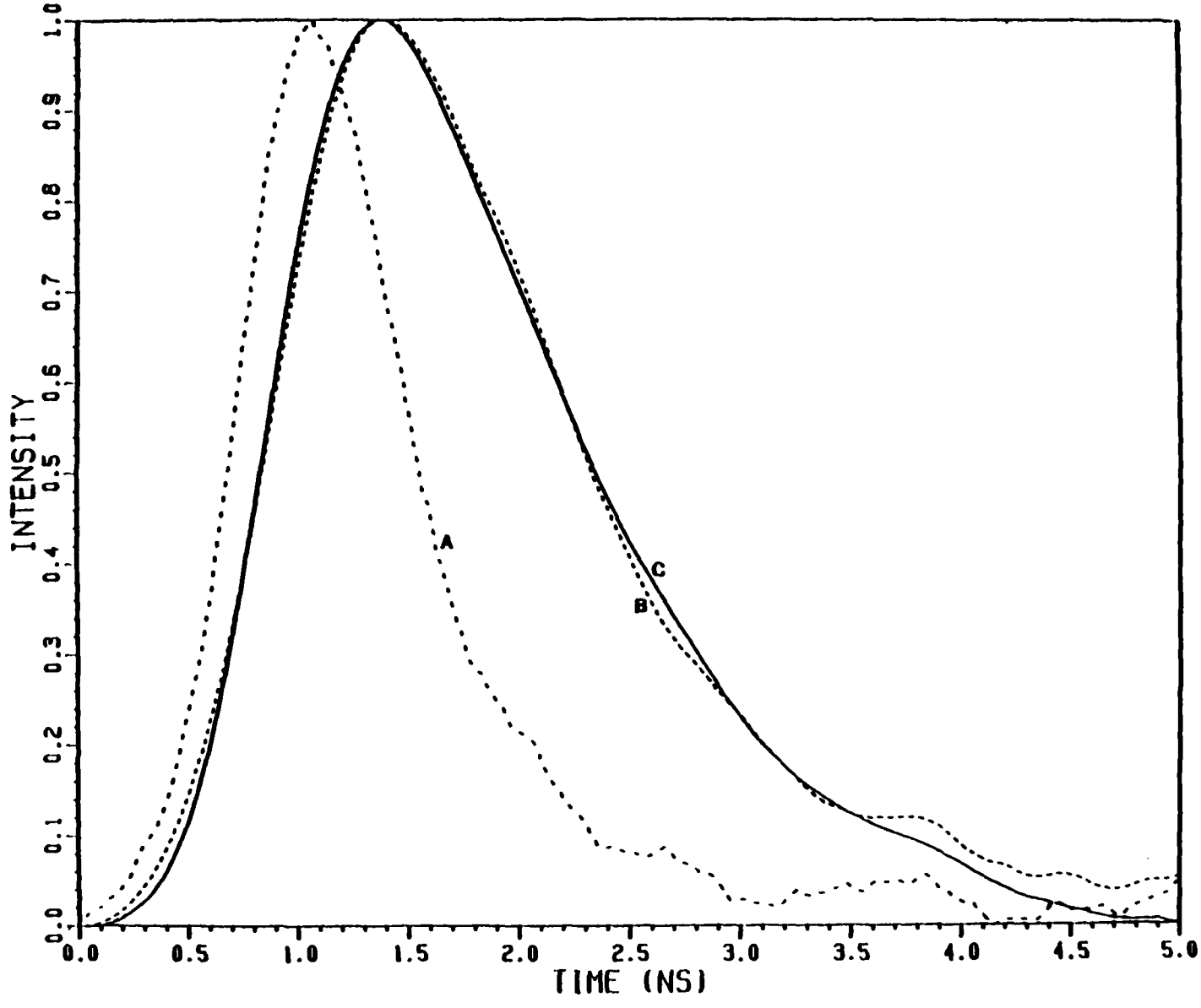
INTENSITY
0.0
0.1
0.2
0.3
0.4
0.5
0.6
0.7
0.8
0.9
1.0
0.0
0.5
1.0
1.5
2.0
2.5
3.0
3.5
4.0
4.5
5.0
TIME (NS)
A
B
C

Fig. 5

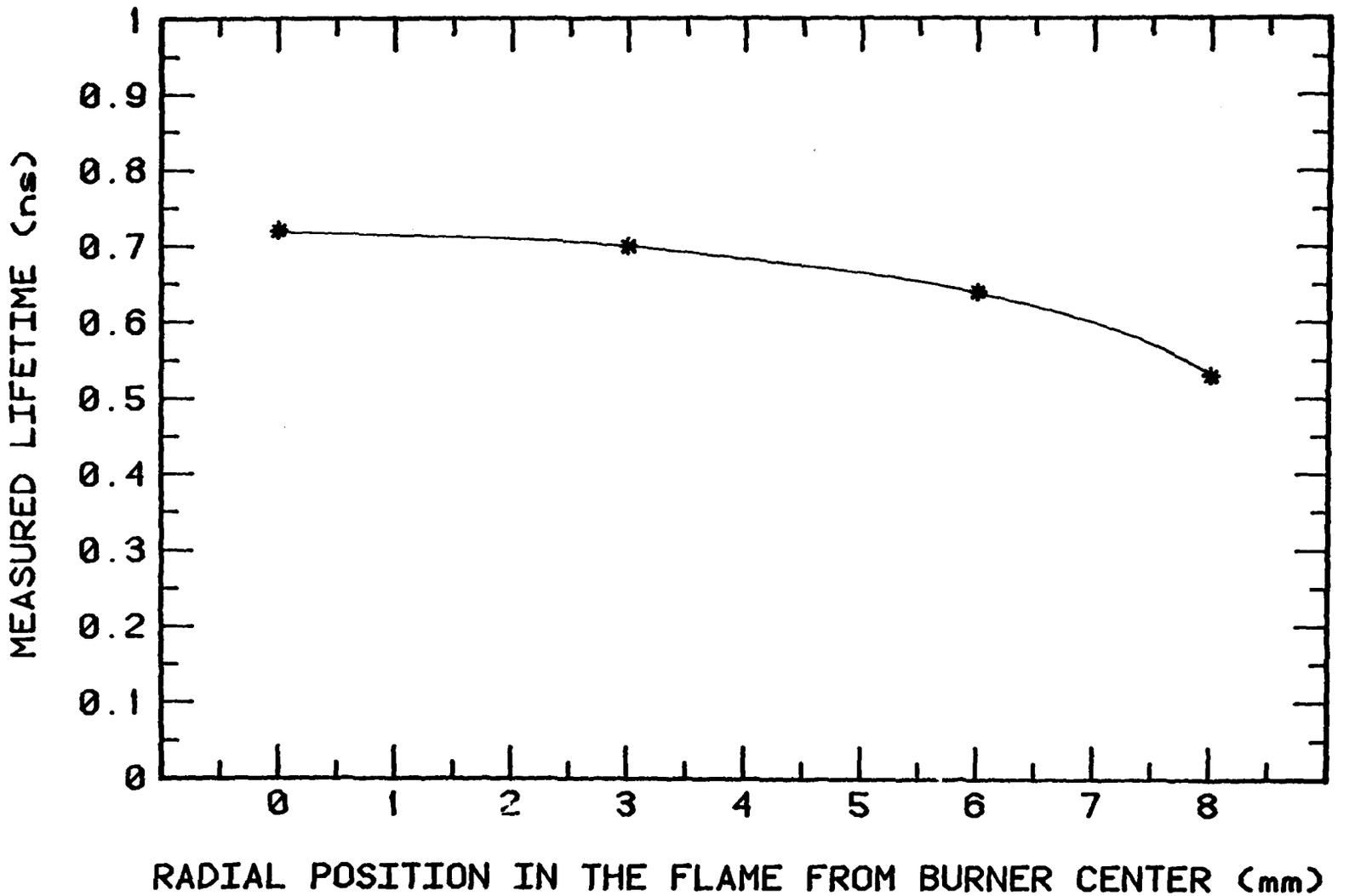
MEASURED LIFETIME (ns)
1
0.9
0.8
0.7
0.6
0.5
0.4
0.3
0.2
0.1
0
0
1
2
3
4
5
6
7
8
RADIAL POSITION IN THE FLAME FROM BURNER CENTER (mm)

Fig 6

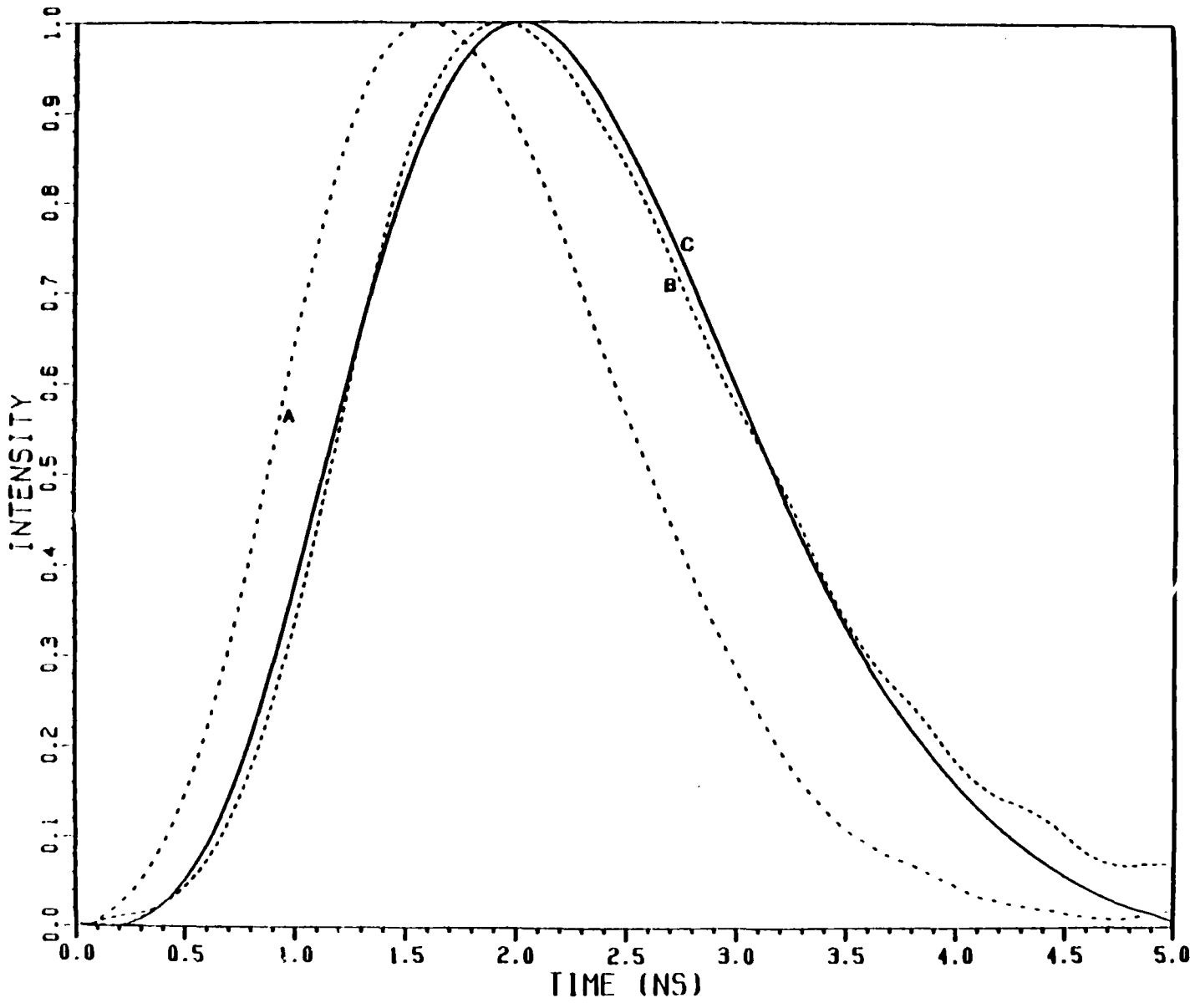
INTENSITY
0.0
0.1
0.2
0.3
0.4
0.5
0.6
0.7
0.8
0.9
1.0
A
B
C
0.0
0.5
1.0
1.5
2.0
2.5
3.0
3.5
4.0
4.5
5.0
TIME (NS)

TECHNICAL REPORT DISTRIBUTION LIST, 051C

	No. Copies
Dr. M. B. Denton Department of Chemistry University of Arizona Tucson, Arizona 85721	1
Dr. R. A. Osteryoung Department of Chemistry State University of New York at Buffalo Buffalo, New York 14214	1
Dr. B. R. Kowalski Department of Chemistry University of Washington Seattle, Washington 98105	1
Dr. S. P. Perone Department of Chemistry Purdue University Lafayette, Indiana 47907	1
Dr. D. L. Venezky Naval Research Laboratory Code 6130 Washington, D.C. 20375	1
Dr. H. Freiser Department of Chemistry University of Arizona Tuscon, Arizona 85721	
Dr. Fred Saalfeld Naval Research Laboratory Code 6110 Washington, D.C. 20375	1
Dr. H. Chernoff Department of Mathematics Massachusetts Institute of Technology Cambridge, Massachusetts 02139	1
Dr. K. Wilson Department of Chemistry University of California, San Diego La Jolla, California	1
Dr. A. Zirino Naval Undersea Center San Diego, California 92132	1
Dr. John Duffin United States Naval Postgraduate School Monterey, California 93940	1
Dr. G. M. Hieftje Department of Chemistry Indiana University Bloomington, Indiana 47401	1
Dr. Victor L. Rehn Naval Weapons Center Code 3813 China Lake, California 93555	1
Dr. Christie G. Enke Michigan State University Department of Chemistry East Lansing, Michigan 48824	1
Dr. Kent Eisentraut, MBT Air Force Materials Laboratory Wright-Patterson AFB, Ohio 45433	1
Walter G. Cox, Code 3632 Naval Underwater Systems Center Building 148 Newport, Rhode Island 02840	1
Professor Isiah M. Warner Texas A&M University Department of Chemistry College Station, Texas 77840	1
Professor George H. Morrison Cornell University Department of Chemisty Ithaca, New York 14853	1
Professor J. Janata Department of Bioengineering University of Utah Salt Lake City, Utah 84112	1
Dr. Carl Heller Naval Weapons Center China Lake, California 93555	1

TECHNICAL REPORT DISTRIBUTION LIST, GEN

	No. Copies
Office of Naval Research Attn: Code 472 800 North Quincy Street Arlington, Virginia 22217	2
ONR Western Regional Office Attn: Dr. R. J. Marcus 1030 East Green Street Pasadena, California 91106	1
ONR Eastern Regional Office Attn: Dr. L. H. Peebles Building 114, Section D 666 Summer Street Boston, Massachusetts 02210	1
Director, Naval Research Laboratory Attn: Code 6100 Washington, D.C. 20390	1
The Assistant Secretary of the Navy (RE&S) Department of the Navy Room 4E736, Pentagon Washington, D.C. 20350	1
Commander, Naval Air Systems Command Attn: Code 310C (H. Rosenwasser) Department of the Navy Washington, D.C. 20360	1
Defense Technical Information Center Building 5, Cameron Station Alexandria, Virginia 22314	12
Dr. Fred Saalfeld Chemistry Division, Code 6100 Naval Research Laboratory Washington, D.C. 20375	1
Mr. James Kelley DTNSRDC Code 2803 Annapolis, Maryland 21402	1
Mr. A. M. Anzalone Administrative Librarian PLASTEC/ARRADCOM Bldg. 3401 Dover, New Jersey 07801	1
U.S. Army Research Office Attn: CRD-AA-IP P.O. Box 1211 Research Triangle Park, N.C. 27709	1
Naval Ocean Systems Center Attn: Mr. Joe McCartney San Diego, California 92152	1
Naval Weapons Center Attn: Dr. A. B. Amster, Chemistry Division China Lake, California 93555	1
Naval Civil Engineering Laboratory Attn: Dr. R. W. Drisko Port Hueneme, California 93401	1
Department of Physics & Chemistry Naval Postgraduate School Monterey, California 93940	1
Scientific Advisor Commandant of the Marine Corps (Code RD-1) Washington, D.C. 20380	1
Naval Ship Research and Development Center Attn: Dr. G. Bosmajian, Applied Chemistry Division Annapolis, Maryland 21401	1
Naval Ocean Systems Center Attn: Dr. S. Yamamoto, Marine Sciences Division San Diego, California 91232	1
Mr. John Boyle Materials Branch Naval Ship Engineering Center Philadelphia, Pennsylvania 19112	1
Dr. L. Jarvis Code 6100 Naval Research Laboratory Washington, D.C. 20375	1

END

DATE
FILMED

11-81

DTIC